






Article

In Vitro Evaluation of the Antimicrobial Properties of Chitosan–Vancomycin Coatings on Grade 4 Titanium Discs: A Preliminary Study

João M. Pinto ¹, Liliana Grenho ^{2,3,*}, Susana J. Oliveira ⁴ , Manuel A. Sampaio-Fernandes ⁴ ,
Maria Helena Fernandes ^{2,3} , Maria Helena Figueiral ^{4,5,*}  and Maria Margarida Sampaio-Fernandes ^{4,5} 

¹ DDM, 4200-060 Porto, Portugal; joaofmdup@gmail.com

² BoneLab, Faculdade de Medicina Dentária, Universidade do Porto, Rua Dr. Manuel Pereira da Silva, 4200-393 Porto, Portugal; mhfernandes@fmd.up.pt

³ LAQV/REQUIMTE, Faculdade de Medicina Dentária, Universidade do Porto, Rua Dr. Manuel Pereira da Silva, 4200-393 Porto, Portugal

⁴ Prosthodontics Department, Faculdade de Medicina Dentária, Universidade do Porto, Rua Dr. Manuel Pereira da Silva, 4200-393 Porto, Portugal; soliveira@fmd.up.pt (S.J.O.); mafernandes@fmd.up.pt (M.A.S.-F.); mfernandes@fmd.up.pt (M.M.S.-F.)

⁵ Instituto de Ciência e Inovação em Engenharia Mecânica e Engenharia Industrial (INEGI), Universidade do Porto, Campus da FEUP, R. Dr. Roberto Frias 400, 4200-465 Porto, Portugal

* Correspondence: lgrenho@fmd.up.pt (L.G.); mhsilva@fmd.up.pt (M.H.F.)

Abstract

Peri-implant infections pose a significant challenge in dental implantology. This study aimed to develop and characterize a chitosan–vancomycin coating for titanium surfaces, focusing on drug loading, release kinetics, antimicrobial performance, and cytocompatibility. Grade 4 titanium discs were coated with a chitosan film using the dip-coating technique and subsequently loaded with vancomycin through immersion in an aqueous solution. Coating morphology was examined by scanning electron microscopy (SEM). Vancomycin loading was quantified by spectrophotometry, and release kinetics were monitored over 144 h (6-day). Antimicrobial activity was assessed through agar diffusion assays against *Staphylococcus aureus*. Cytocompatibility was evaluated using human mesenchymal stem cells (hMSCs), whose metabolic activity, adhesion, and morphology were assessed over a 19-day culture period by resazurin assay and SEM. SEM analysis revealed a uniformly distributed, smooth, and crack-free chitosan film, which remained stable after drug loading. The coating exhibited a biphasic release profile, characterized by an initial burst followed by sustained release over six days, which maintained antimicrobial activity, as confirmed by inhibition zones. hMSCs adhered and proliferated on the coated surfaces, displaying normal morphology despite a transient reduction in metabolic activity on vancomycin-containing films. These findings support the potential of chitosan–vancomycin coatings as localized antimicrobial strategies for implant applications, warranting further in vivo and mechanical evaluations.



Academic Editor: Seunghan Oh

Received: 30 July 2025

Revised: 3 January 2026

Accepted: 5 January 2026

Published: 8 January 2026

Copyright: © 2026 by the authors.

Licensee MDPI, Basel, Switzerland.

This article is an open access article distributed under the terms and conditions of the [Creative Commons Attribution \(CC BY\)](https://creativecommons.org/licenses/by/4.0/) license.

Keywords: dental implants; titanium; peri-implantitis; chitosan; vancomycin; coating; antimicrobial; cytocompatibility

1. Introduction

Dental implants have become a widely adopted solution for rehabilitating edentulous patients, offering reliable restoration of masticatory function and aesthetics. This success

is largely attributed to titanium, which presents excellent chemical stability, mechanical strength, favourable physical properties, and high biocompatibility with surrounding tissues [1,2]. Titanium is widely used for dental implants also due to its lightweight nature, resistance to fatigue and corrosion, formation of a protective oxide layer (TiO₂) that ensures long-term durability, and the possibility of surface modification to enhance performance [3]. However, the increasing use of dental implants has been accompanied by a growing incidence of peri-implant diseases, particularly peri-implantitis and mucositis, both characterized by inflammatory disorders affecting the peri-implant hard and soft tissues. Reported prevalence rates range from 20% to 40% [1,4]. Interpretation of implant failure rates remains complex due to variability in surgical techniques, follow-up duration, and inconsistent definitions of clinical success [5].

Peri-implantitis is primarily driven by the accumulation of bacterial biofilms on the implant surface, leading to progressive bone loss and potential implant failure [6]. This condition is associated with elevated levels of periodontopathogenic microorganisms, such as *Porphyromonas gingivalis*, *Treponema denticola*, and *Tannerella forsythia* [7]. Although *Staphylococcus aureus* is not a classical periodontal pathogen, it plays an important role as an early colonizer of implant surfaces, creating a favourable microenvironment that facilitates subsequent colonization by more virulent species [8,9].

In response to these microbial challenges, current strategies for titanium implant surface modification aim not only to promote osseointegration but also to provide effective and durable antimicrobial protection [10,11]. Three main categories of coatings have been identified: antibacterial peptides, synthetic antimicrobial molecules (e.g., polymers and antibiotics), and metallic nanoparticles (e.g., silver). These coatings employ the prevention of bacterial adhesion (anti-adhesive), contact-mediated bactericidal effects (contact-killing), and the controlled release of antimicrobial agents (release-killing) [1,11]. Passive anti-adherent coatings—such as polymers, hydrogels, polymeric multilayers, and textured surfaces—prevent the initial bacterial adhesion, but their long-term stability and effectiveness tend to diminish upon exposure to the physiological environment [11]. In contrast, active bactericidal coatings exert antimicrobial effects either through direct contact with the material surface or via controlled release of antimicrobial agents. These coatings can provide short-, medium-, or long-term bactericidal activity, and include positively charged polymers, peptides, metal nanoparticles, antibiotics, and antiseptics [11].

For successful clinical translation, antimicrobial coatings must meet several essential criteria: they should preserve the implant's mechanical and physicochemical integrity, exhibit no cytotoxicity toward host tissues, and provide sustained antimicrobial activity [12,13]. Several techniques are available for applying antimicrobial coatings to implant surfaces, including dip coating, chemical deposition, and electrophoretic deposition [1]. Dip coating is particularly attractive due to its simplicity, cost-effectiveness, and ability to produce uniform, thin films on titanium substrates while enabling the sustained release of antimicrobial agents [14]. Among the various systems under investigation, chitosan has been widely explored; however, its intrinsic antibacterial activity is insufficient to provide effective protection against implant-associated infections [11]. Nevertheless, chitosan has shown significant potential as a vehicle for delivering antimicrobial agents due to its biocompatibility, film-forming ability, and controlled release properties [14]. Incorporating a bioactive vancomycin-loaded coating onto titanium implants can improve both osseointegration and antibacterial efficacy by enabling localized, sustained antibiotic delivery [15–21]. Consequently, chitosan–vancomycin combinations represent a promising strategy for developing localized drug-delivery coatings aiming at preventing implant-associated infections in orthopaedic or dental applications [22–24].

The present study aims to evaluate the antimicrobial potential of a chitosan–vancomycin coating applied to grade 4 titanium discs using a dip coating technique. Specifically, the study focuses on (1) assessing chitosan’s ability to enable vancomycin loading and release; (2) characterizing the temporal profile of vancomycin release; (3) determining the *in vitro* antimicrobial activity of the coated titanium discs and the released vancomycin against *S. aureus*; and (4) evaluating cytocompatibility to human mesenchymal stem cells.

2. Materials and Methods

2.1. Preparation of Titanium Discs

This *in vitro* experimental study used commercially pure grade 4 titanium discs (Lot: 60018, Klockner[®], Barcelona, Spain) with no prior surface treatment. Each disc had an approximate area of 0.64 cm². Prior to the experimental procedures, all discs were cleaned in an ultrasonic bath (Sonorex Super RK 100, Bandelin[®], Mecklenburg-Vorpommern, Germany) using acetone (Juliette[®], Valencia, Spain) and ethanol (AGA[®], São Brás de Alportel, Portugal) for 10 min each, to remove surface contaminants. The discs were then rinsed with distilled water and dried at 37 °C for 2 h. Samples were randomly assigned to three experimental groups (EGs) based on surface treatment: EG1—uncoated titanium discs; EG2—titanium discs coated with a chitosan film; and EG3—titanium discs coated with a chitosan film and loaded with vancomycin.

2.2. Synthesis and Application of Chitosan Coating

Chitosan films were prepared following a protocol adapted from Vakili et al. [25], based on the procedure by Zhang et al. [26]. High-molecular-weight chitosan (degree of deacetylation $\geq 75\%$, Sigma-Aldrich[®], Taufkirchen, Germany) was dissolved in acetic acid (Sigma-Aldrich[®], Germany) at a concentration of 0.5% (*w/v*) and stirred for 12 h. Separately, 0.4 g of glycerol (Acofarma[®], Barcelona, Spain) was dispersed in 80 mL of 1% (*v/v*) acetic acid and stirred for 12 h at 4 °C. The chitosan solution was then added to the glycerol–acetic acid mixture under continuous stirring to form the final coating solution. Discs in EG2 and EG3 were coated using a dip-coating technique. Each disc was immersed in 2 mL of the coating solution for 1 min, followed by air-drying under a fume hood at room temperature for 12 h to ensure uniform film formation and avoid deformation.

2.3. Vancomycin Loading onto Chitosan-Coated Titanium Discs

Chitosan-coated discs were immersed in an aqueous vancomycin hydrochloride solution (25 mg/mL, pH 4, Laboratórios Normon[®], Lisbon, Portugal) and incubated at 37 °C for 12 h with agitation at 120 rpm using an orbital shaker. After incubation, the discs were rinsed with distilled water, air-dried, and stored in a desiccator until further analysis.

2.4. Surface Characterization

The surface morphology of uncoated titanium discs, chitosan-coated discs, and chitosan-coated discs subsequently loaded with vancomycin was examined by scanning electron microscopy (SEM) using a Quanta 400 FEG/ESEM microscope (FEI, Hillsboro, OR, USA). Three independent samples per group were analysed to assess coating distribution and morphological integrity.

2.5. Quantification of Loaded Vancomycin

To quantify the amount of vancomycin loaded onto the chitosan-coated discs, each sample was immersed in 1 mL of 0.5% (*v/v*) acetic acid (*n* = 5). Tubes were incubated at 37 °C with constant agitation at 150 rpm for 2 h. The absorbance of the resulting so-

lutions was measured at 280 nm using a microplate reader (Synergy HT, BioTek®, Bad Friedrichshall, Germany). Vancomycin concentration was determined using a previously established calibration curve. Drug loading of vancomycin refers to the amount of vancomycin incorporated into the chitosan coating on the titanium surface, and the loaded vancomycin was determined following the equation:

$$\text{Loaded vancomycin} = (\text{total amount of vancomycin} - \text{amount of free vancomycin in the solution}) / (\text{total amount of vancomycin})$$

2.6. Vancomycin Release Kinetics

To evaluate vancomycin release over time, discs (EG3, n = 5) were individually immersed in 1 mL of phosphate-buffered saline (PBS, Fisher Scientific®, Suwanee, GA, USA) and incubated at 37 °C with continuous shaking at 120 rpm. At predefined time points (0.5, 1, 1.5, 2, 3, 6, 24, 48, and 144 h), 100 µL aliquots were collected from the supernatant and replaced with an equal volume of fresh PBS to maintain sink conditions. Absorbance at 280 nm was measured, and vancomycin concentrations were calculated from the calibration curve.

2.7. Antimicrobial Activity of Coated Titanium Discs

The antimicrobial effect of the vancomycin-loaded chitosan coating (EG3, n = 5) was evaluated using the Kirby–Bauer disk diffusion method. A standardized suspension of *Staphylococcus aureus* ATCC 25923 (ca. 10⁸ CFU/mL) was prepared using spectrophotometric calibration (600 nm) and uniformly swabbed onto Mueller–Hinton agar plates. Ti-discs were gently pressed onto the agar and incubated at 37 °C in the dark to prevent any potential photocatalytic effects from titanium. After 24 h, the diameter of the inhibition zones surrounding each disc was measured.

2.8. Antimicrobial Activity of Released Vancomycin

Aliquots collected during the release assay were tested using the Kirby–Bauer method to evaluate the bioactivity of vancomycin released from the coating over time. Sterile paper discs (5 mm) were impregnated with 10 µL of each release sample and placed onto agar plates previously inoculated with *S. aureus*, as previously described. Paper discs impregnated with 10 µL of the 25 mg/mL vancomycin solution served as positive control, while discs treated with 0.5% (v/v) acetic acid and PBS (10 µL) were used to rule out interference from these reagents. After 24 h of incubation at 37 °C, inhibition zones were measured.

2.9. Cytocompatibility Study

The cytocompatibility of the vancomycin-loaded chitosan coating (EG3) was evaluated in vitro using human mesenchymal stem cells (hMSCs; Catalog No. PT-2501, Lonza, Basel, Switzerland). For comparison, samples from groups EG1 and EG2 were also included. hMSCs were cultured in α -Minimum Essential Medium (α -MEM), supplemented with 10% fetal bovine serum, 50 µg/mL ascorbic acid, 100 U/mL penicillin, 100 µg/mL streptomycin, and 0.25 µg/mL amphotericin B (all reagents from Gibco, Waltham, MA, USA). Cultures were maintained at 37 °C in a humidified atmosphere containing 5% CO₂. Discs from each experimental group were seeded at 2 × 10⁴ cells/cm² and cultured for up to 19 days. At predetermined time points, cultures established on the disc surfaces were evaluated regarding cell metabolic activity using the resazurin assay and cell adhesion and morphology by SEM. For the resazurin assay, seeded discs were incubated for 3 h at 37 °C in fresh medium containing 10% resazurin solution (0.1 mg/mL, Sigma-Aldrich, St. Louis, MO, USA). Fluorescence intensity of the medium was then measured at excitation and

emission wavelengths of 530 nm and 590 nm, respectively. Values were normalized to those of the control group (EG1). For SEM analysis, cell-seeded discs were fixed with 1.5% glutaraldehyde (Sigma-Aldrich, St. Louis, MO, USA) for 15 min, dehydrated through a graded ethanol series (50 to 100%), critical-point dried, and sputter-coated with a gold-palladium film prior to imaging with a Quanta 400 FEG/ESEM microscope (FEI, Hillsboro, OR, USA).

2.10. Statistical Analysis

Data are presented as mean \pm standard deviation (SD). Statistical analyses were performed using one-way analysis of variance (ANOVA), followed by Tukey's post hoc test (SPSS software, Version 30.0.0.0, IBM, Armonk, NY, USA). Differences were considered statistically significant at $p < 0.05$.

3. Results

3.1. Surface Characterization

SEM analysis was performed to evaluate the surface characteristics, uniformity, and stability of the chitosan coating before and after vancomycin loading. Representative images are shown in Figure 1. EG1 displayed the typical grooved microtopography of machined titanium. In EG2, the chitosan film appeared uniformly distributed across the surface, forming a smooth, continuous layer without cracks. The underlying titanium morphology remained partially discernible, indicating that the coating was extremely thin. Following vancomycin loading (EG3), the coating preserved its integrity and surface continuity. The representative EG3 image was intentionally selected from a coating–substrate transition area to highlight the low thickness of the deposited chitosan film.

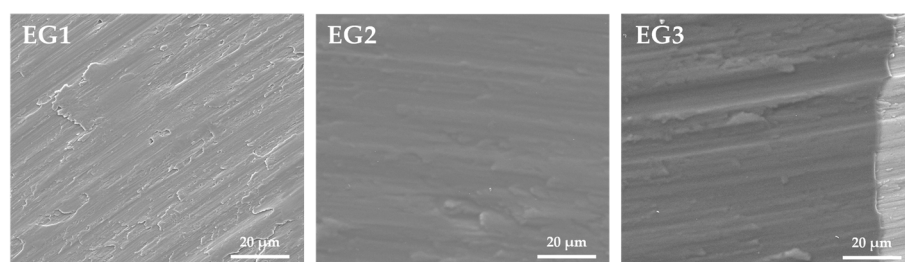


Figure 1. SEM micrographs of surface morphology of uncoated titanium discs (EG1), titanium discs coated with a chitosan film (EG2), and titanium discs coated with a chitosan film and subsequently loaded with vancomycin (EG3) (high voltage: 10 kV; 2500 \times).

3.2. Vancomycin Loaded onto Chitosan-Coated Titanium Discs

The vancomycin concentration loaded onto the chitosan-coated titanium discs (EG3) was $84.4 \pm 9.8 \mu\text{g/mL}$, corresponding to 0.34% of the drug content retained on the chitosan-coated titanium discs. This was approximately $131.9 \mu\text{g/cm}^2$.

3.3. Vancomycin Release Kinetics

The cumulative release of vancomycin from chitosan-coated titanium discs over 144 h (6 days) is illustrated in Figure 2. A rapid initial burst release occurred within the first 30 min, reaching $48.9 \mu\text{g/mL}$, which corresponded to approximately 50% of the total drug load. This was followed by a slower, sustained release phase, with concentrations reaching $73.7 \mu\text{g/mL}$ at 3 h (representing 78% of the total load) and gradually approaching a plateau toward later time points, indicating near-complete elution of the antibiotic.

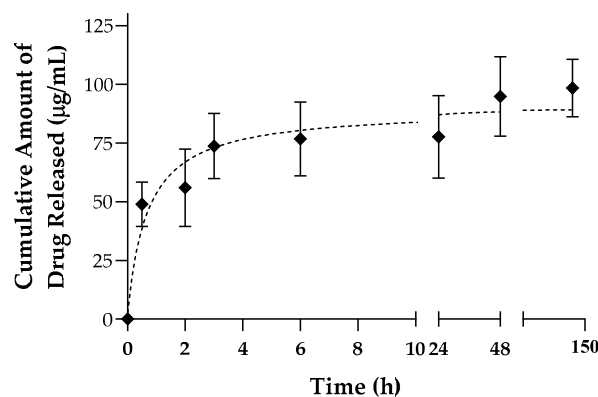
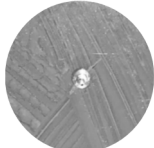
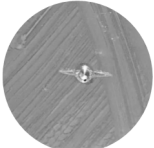
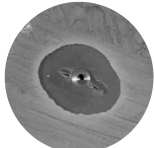


Figure 2. Cumulative release kinetics of vancomycin from chitosan-coated titanium discs over 144 h. The dotted line represents nonlinear regression fitting.

3.4. Antimicrobial Activity of Coated Titanium Discs

The antimicrobial efficacy of the titanium discs was assessed by measuring the inhibition zones formed by *S. aureus* after 24 h of incubation (Table 1). No inhibition zones were detected around uncoated titanium discs (EG1) or those coated with chitosan film (EG2). In contrast, discs coated with chitosan and loaded with vancomycin (EG3) produced distinct inhibition zones, with an average diameter of 17 ± 0.5 mm.

Table 1. Inhibition zones formed by *S. aureus* after 24 h of incubation with titanium discs from the three experimental groups, accompanied by illustrative macroscopic images of the corresponding inhibition zones.

| | EG1 | EG2 | EG3 |
|--|---|---|---|
| Inhibition zones (mean \pm SD ¹ , mm) | 0 | 0 | 17 ± 0.5 |
| Macroscopic image |  |  |  |

EG1: uncoated titanium discs; EG2: chitosan-coated discs; EG3: chitosan-coated discs loaded with vancomycin.
¹ SD—standard deviation.

3.5. Antimicrobial Activity of Released Vancomycin

The antimicrobial activity of vancomycin released from the coated discs was evaluated using paper discs impregnated with samples (10 μ L) collected during the release assay. All samples inhibited *S. aureus* growth, with average inhibition zones of approximately 7.0 mm (Table 2). The largest inhibition zones were observed during the initial release phase (0.5–1 h). The positive control (25 mg/mL vancomycin) produced inhibition zones averaging 20 ± 0.3 mm, while no inhibition zones were detected in negative controls (acetic acid and PBS).

3.6. Cytocompatibility Study

Human mesenchymal stem cells (hMSCs) were used to evaluate the cytocompatibility of the vancomycin-loaded chitosan coating. Cell metabolic activity, measured using the resazurin assay, is presented in Figure 3a. hMSCs cultured on Ti-coated discs (EG2 and EG3) exhibited significantly lower metabolic activity than those in the control group (EG1). Despite this reduction, cells on both coated surfaces demonstrated progressive proliferation over the 19-day culture period. Notably, by day 19, metabolic activity in the EG2 group had

reached levels comparable to those of the control. In the EG3 group, the presence of vancomycin resulted in an overall decrease in metabolic activity; however, cells retained their proliferative capacity and gradually overcame the initial inhibitory effects over time. SEM analysis provided additional insights into cell morphology and cell–material interactions (Figure 3b). After 15 days, hMSCs on all surfaces displayed well-spread morphologies, with confluent layers and elongated cell shapes indicative of favourable adhesion and proliferation. In particular, cells on EG3 discs exhibited pronounced filopodia extensions, suggesting strong anchorage and close interaction with the coated surface.

Table 2. Inhibition zones formed by *S. aureus* after 24 h of incubation with paper discs impregnated with vancomycin-containing eluates at various time points.

| Time-Point (h) | Inhibition Zone (Mean \pm SD ¹ , mm) |
|----------------|---|
| 0.5 | 7.7 \pm 0.5 |
| 1 | 8.0 \pm 0.1 |
| 1.5 | 7.3 \pm 0.5 |
| 2 | 6.7 \pm 0.5 |
| 3 | 7.3 \pm 0.9 |
| 6 | 6.7 \pm 0.9 |
| 24 | 6.3 \pm 0.5 |
| 48 | 6.7 \pm 0.9 |
| 144 | 6.3 \pm 0.9 |

¹ SD—standard deviation.

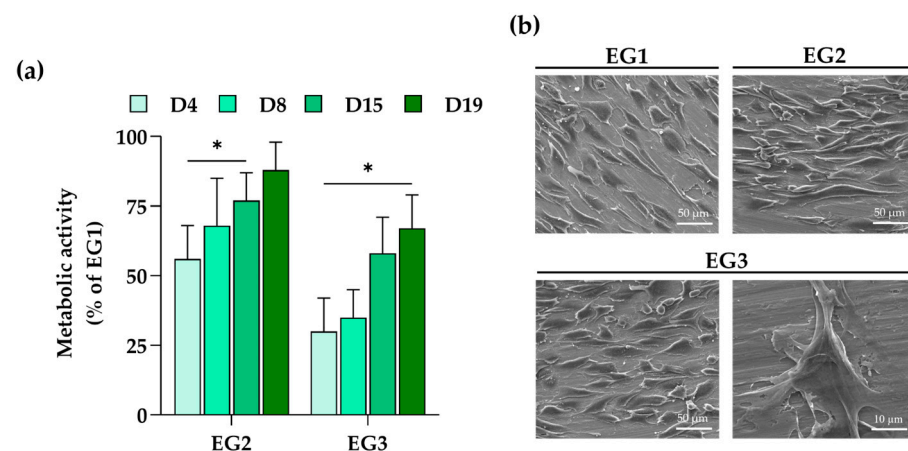


Figure 3. (a) Metabolic activity of hMSCs cultured on the discs for 19 days, assessed by the resazurin assay. Values were normalized to the EG1 group (control). * Significantly different from the control ($p < 0.05$). (b) Representative SEM images of hMSC morphology and surface distribution after 15 days of culture.

4. Discussion

Peri-implant infections remain a significant challenge in dental implantology. Bacterial colonization and biofilm formation on implant surfaces can jeopardize osseointegration and compromise the long-term success of implant-supported rehabilitations [27]. A promising strategy to mitigate this risk involves the surface modification of implants with antimicrobial coatings capable of releasing antimicrobial agents locally, thereby reducing early bacterial adhesion and subsequent infection. In this context, the present in vitro study investigated the performance of a chitosan–vancomycin coating applied to grade 4 titanium discs using the dip coating technique, with a specific focus on drug loading efficiency, release kinetics, antimicrobial activity against *S. aureus*, and cytocompatibility to

human mesenchymal stem cells. SEM surface characterization confirmed the successful formation of the coating system. Uncoating titanium discs displayed the characteristic microtopography associated with their manufacturing process, consistent with previous reports [28]. Chitosan-coated discs (EG2) and those additionally loaded with vancomycin (EG3) exhibited uniform and continuous film coverage; however, the underlying titanium microtopography remained discernible, indicating that the deposited films were extremely thin. The addition of glycerol as a plasticizer likely enhanced film flexibility, contributing to the formation of crack-free coatings. Additionally, the smooth and homogeneous appearance of the chitosan layer can be attributed to the high solubility of chitosan in acetic acid, which promotes the formation of a true solution rather than a suspension and thus prevents the fibrous or particulate morphologies often observed with less soluble formulations [29].

Regarding vancomycin release, the results demonstrated that chitosan effectively facilitated vancomycin loading and sustained release over a 6-day period, with confirmed antimicrobial efficacy against *S. aureus*.

Vancomycin, a glycopeptide antibiotic, exhibits broad-spectrum activity and is especially effective against Gram-positive pathogens commonly involved in early implant colonization [30,31]. Its high molecular weight, stability, and limited systemic absorption make it particularly suitable for localized delivery applications [32]. Chitosan was selected as the drug carrier due to its favourable properties, including biocompatibility, film-forming ability, and intrinsic, albeit limited, antimicrobial activity [33]. Additionally, chitosan's amino groups (-NH₂) can interact ionically with vancomycin's phenolic groups, potentially enhancing drug loading [14,34]. Despite these chemical affinities, the vancomycin loading observed in this study was relatively low, with only 0.34% of the initial drug content retained on the chitosan-coated titanium discs. While the relatively low chitosan concentration may limit the total amount of vancomycin that can be incorporated, the chitosan concentration and glycerol formulation used (as per the protocol of Zhang et al. [26]) ensured homogeneous coating and reproducible drug release. This low result contrasts with previous reports, such as those by Cao and Sun, which achieved higher drug loading efficiencies of rifampicin onto chitosan films [34]. The discrepancy may be attributed to differences in methodology, namely the use of methanol as solvent in their study, which likely increased drug solubility and loading efficiency [35]. Additional factors, including sample geometry, film thickness, and incubation conditions, may have also contributed to variations in loading outcomes. Although the present study shows a uniform film by SEM, slight thickness differences inherent to dip-coating could still contribute to variability in drug loading and release kinetics. Thicker films may hold more vancomycin but may slow diffusion, whereas thinner coatings load less drug and release it more rapidly. Thus, controlling thickness is important for achieving consistent release kinetics.

The vancomycin release profile exhibited a biphasic pattern, typical of polymer-based drug delivery systems [36]. An initial burst release occurred within the first 30 min, accounting for approximately 50% of the total drug load (48.9 µg/mL). This rapid release likely reflects the surface-bound nature of vancomycin, providing immediate antimicrobial activity. This was followed by a slower, sustained release phase, extending up to 3 h (reaching a concentration of up to 73.7 µg/mL), consistent with diffusion-controlled release from the deeper layers of the chitosan matrix. Such a release profile is advantageous, as it maintains therapeutic concentrations during the critical early period (up to 6 h) when bacterial adhesion and early biofilm formation are most likely to occur [34,37,38]. Importantly, the system continued to release vancomycin at bactericidal levels beyond this time window, potentially providing protection against both early and delayed bacterial colonization [39,40]. By the final time points, vancomycin release approached near-complete delivery. In contrast to the findings of the present study, Swanson et al. reported an

extremely rapid vancomycin release (95% within 5 min) from titanium alloy rods (Ti6Al4V) coated with chitosan [39]. Their protocol, based on brief immersion in a highly concentrated vancomycin solution, resulted in poor drug retention and minimal sustained release, suggesting that formulation parameters play a pivotal role in controlling release kinetics. Nevertheless, in the present study, the determination of the drug release kinetics was only performed in PBS, thus at a neutral pH, which is a limitation. In vivo, pH fluctuations may significantly influence the release kinetics of chitosan–vancomycin coatings. Chitosan is pH-responsive, and acidic environments, such as those found in peri-implant tissues during inflammation or early infection, can increase chitosan swelling and accelerate the release of vancomycin. In contrast, neutral or slightly alkaline conditions may slow down the diffusion process. This pH dependence underscores the importance of characterizing release kinetics within physiologically relevant pH ranges to more accurately predict in vivo performance.

Maintaining therapeutic antibiotic concentrations is crucial, particularly in the face of increasing antimicrobial resistance. *S. aureus* strains classified as vancomycin-sensitive (VSSA) typically respond to concentrations of 2–4 µg/mL, while vancomycin-intermediate *S. aureus* (VISA) and vancomycin-resistant *S. aureus* (VRSA) require significantly higher levels, ranging from 4–8 µg/mL and above 16 µg/mL, respectively [41]. The vancomycin concentrations released in this study consistently exceeded these thresholds, highlighting the potential of this system to address infections caused by both susceptible and resistant phenotypes.

The antimicrobial activity of the coating was confirmed by agar diffusion assays, where inhibition zones were observed around both the vancomycin-loaded titanium discs and paper discs impregnated with the released antibiotic, further demonstrating the bioactivity of the released drug. In contrast, uncoated discs and those coated solely with chitosan showed no inhibition zones, indicating that chitosan alone did not provide sufficient antibacterial effect under the test conditions. This observation is consistent with previous findings, including those reported by Cao and Sun, which found that chitosan did not inhibit bacterial growth [34]. The lack of antimicrobial activity may be attributed to factors such as the molecular weight of chitosan, its degree of deacetylation, or the absence of chemical functionalization. Notably, chemical modifications—such as substituting -OH groups with -CH₂COOH groups—have been shown to enhance chitosan's antimicrobial properties [14].

In addition to assessing antimicrobial performance, the cytocompatibility of the vancomycin-loaded chitosan coating was evaluated using human mesenchymal stem cells (hMSCs). These cells are particularly suitable for cytocompatibility studies due to their sensitivity to environmental cues and their relevance in tissue regeneration, allowing them to more accurately mimic in vivo responses than other cell types [42]. In the present study, hMSCs cultured on the EG2 and EG3 groups exhibited lower metabolic activity than those on the non-coated titanium control (EG1). This decrease may be related to the high degree of deacetylation of the chitosan employed, which has been reported to potentially delay early cell attachment and proliferation [43]. Nevertheless, despite the initial delay, hMSCs adhered and proliferated on both coated surfaces, suggesting that the material did not induce persistent cytotoxicity. The presence of vancomycin in the EG3 coating further delayed early cell proliferation, consistent with previous reports demonstrating that high local concentrations of vancomycin can adversely affect eukaryotic cell viability [44]. This transient inhibitory effect is likely associated with localized antibiotic accumulation at the material interface upon initial cell seeding. Importantly, metabolic activity gradually recovered over time, suggesting that hMSCs adapted to the local environment and were able to resume active proliferation.

Overall, although preliminary, these findings provide encouraging evidence that the proposed chitosan–vancomycin coating achieves a balance between antimicrobial activity and cytocompatibility, supporting its potential for application in infection-prone implantable devices, such as dental implants. Future studies should investigate the coating against a wider range of peri-implant pathogens and assess its osteogenic potential and mechanical stability under physiological conditions to further advance its commercial and clinical prospects. Key challenges include achieving scalable, reproducible manufacturing, maintaining coating stability during implantation, and precisely controlling drug-release kinetics. Additional difficulty involves regulatory considerations related to vancomycin use, as well as demonstrating sterilization compatibility, long-term stability, and consistent in vivo performance.

5. Conclusions

This preliminary study successfully demonstrated the production of chitosan-coated titanium discs capable of effective vancomycin loading and sustained release. The system exhibited a biphasic drug release profile, characterized by an initial burst followed by a slower, sustained release lasting up to 144 h (6 days). This release pattern maintained antimicrobial concentrations adequate to inhibit *S. aureus*, indicating potential to prevent both early-stage bacterial adhesion and delayed biofilm formation on titanium implant surfaces. Moreover, cytocompatibility assessments confirmed that hMSCs could adhere and proliferate on the coated surfaces, supporting the biological feasibility of this approach. Overall, these findings underscore the potential of this chitosan–vancomycin coating as a localized drug delivery strategy for reducing the risk of peri-implant infections. Further investigations, including extended in vitro testing and in vivo validation, are necessary to assess its long-term functional performance, biocompatibility, and clinical applicability.

Author Contributions: Conceptualization, J.M.P., M.H.F. (Maria Helena Fernandes) and M.M.S.-F.; methodology, L.G. and M.H.F. (Maria Helena Figueiral); investigation, J.M.P. and L.G.; writing—original draft preparation, J.M.P., M.M.S.-F. and L.G.; writing—review and editing, S.J.O., M.A.S.-F. and M.H.F. (Maria Helena Fernandes); supervision, M.H.F. (Maria Helena Figueiral), M.H.F. (Maria Helena Fernandes) and M.M.S.-F. All authors have read and agreed to the published version of the manuscript.

Funding: This research received no external funding.

Institutional Review Board Statement: Not applicable.

Informed Consent Statement: Not applicable.

Data Availability Statement: Data is contained within the article.

Acknowledgments: In this section, we acknowledge the support given by Klockner S.A. (donation of titanium discs used for experiments).

Conflicts of Interest: The authors declare no conflicts of interest.

References

1. Chen, Z.; Wang, Z.; Qiu, W.; Fang, F. Overview of Antibacterial Strategies of Dental Implant Materials for the Prevention of Peri-Implantitis. *Bioconjug. Chem.* **2021**, *32*, 627–638. [[CrossRef](#)]
2. Spriano, S.; Yamaguchi, S.; Bairo, F.; Ferraris, S. A critical review of multifunctional titanium surfaces: New frontiers for improving osseointegration and host response, avoiding bacteria contamination. *Acta Biomater.* **2018**, *79*, 1–22. [[CrossRef](#)]
3. Nicholson, J.W. Titanium Alloys for Dental Implants: A Review. *Prosthesis* **2020**, *2*, 100–116. [[CrossRef](#)]
4. Renvert, S.; Lindahl, C.; Persson, G.R. Occurrence of cases with peri-implant mucositis or periimplantitis in a 21–26 years follow-up study. *J. Clin. Periodontol.* **2018**, *45*, 233–240. [[CrossRef](#)]

5. Simonis, P.; Dufour, T.; Tenenbaum, H. Long-term implant survival and success: A 10–16-year follow-up of non-submerged dental implants. *Clin. Oral Implants Res.* **2010**, *21*, 772–777. [[CrossRef](#)] [[PubMed](#)]
6. Berglundh, T.; Armitage, G.; Araujo, M.G.; Avila-Ortiz, G.; Blanco, J.; Camargo, P.M.; Chen, S.; Cochran, D.; Derks, J.; Figuero, E.; et al. Peri-implant diseases and conditions: Consensus report of workgroup 4 of the 2017 World Workshop on the Classification of Periodontal and Peri-Implant Diseases and Conditions. *J. Periodontol.* **2018**, *89*, S313–S318. [[CrossRef](#)]
7. Odatsu, T.; Kuroshima, S.; Sato, M.; Takase, K.; Valanezhad, A.; Naito, M.; Sawase, T. Antibacterial Properties of Nano-Ag Coating on Healing Abutment: An In Vitro and Clinical Study. *Antibiotics* **2020**, *9*, 347. [[CrossRef](#)] [[PubMed](#)]
8. Socransky, S.S.; Haffajee, A.D. Periodontal microbial ecology. *Periodontol.* **2000** **2005**, *38*, 135–187. [[CrossRef](#)] [[PubMed](#)]
9. Salvi, G.E.; Fürst, M.M.; Lang, N.P.; Persson, G.R. One-year bacterial colonization patterns of *Staphylococcus aureus* and other bacteria at implants and adjacent teeth. *Clin. Oral Implants Res.* **2008**, *19*, 242–248. [[CrossRef](#)]
10. Palla-Rubio, B.; Araújo-Gomes, N.; Fernández-Gutiérrez, M.; Rojo, L.; Suay, J.; Gurruchaga, M.; Goñi, I. Synthesis and Characterization of Silica Chitosan Hybrid Materials as Antibacterial Coatings for Titanium Implants. *Carbohydr. Polym.* **2019**, *203*, 331–341. [[CrossRef](#)]
11. Teulé-Trull, M.; Altuna, P.; Arregui, M.; Rodríguez-Ciurana, X.; Aparicio, C. Antibacterial coatings for dental implants: A systematic review. *Dent. Mater.* **2025**, *41*, 229–247. [[CrossRef](#)]
12. Fenton, O.S.; Olafson, K.N.; Pillai, P.S.; Mitchell, M.J.; Langer, R. Advances in Biomaterials for Drug Delivery. *Adv. Mater.* **2018**, *7*, e1705328. [[CrossRef](#)]
13. Pokrowiecki, R. The paradigm shift for drug delivery systems for oral and maxillofacial implants. *Drug Deliv.* **2018**, *25*, 1504–1515. [[CrossRef](#)]
14. Teixeira-Santos, R.; Lima, M.; Gomes, L.C.; Mergulhão, F.J. Antimicrobial coatings based on chitosan to prevent implant-associated infections: A systematic review. *iScience* **2021**, *24*, 103480. [[CrossRef](#)] [[PubMed](#)]
15. Yang, C.C.; Lin, C.C.; Liao, J.W.; Yen, S.K. Vancomycin-chitosan composite deposited on post porous hydroxyapatite coated Ti6Al4V implant for drug controlled release. *Mater. Sci. Eng. C Mater. Biol. Appl.* **2013**, *33*, 2203–2212. [[CrossRef](#)]
16. Suchý, T.; Vištejnová, L.; Šupová, M.; Klein, P.; Bartoš, M.; Kolinko, Y.; Blassová, T.; Tonar, Z.; Pokorný, M.; Sucharda, Z.; et al. Vancomycin-Loaded Collagen/Hydroxyapatite Layers Electrospun on 3D Printed Titanium Implants Prevent Bone Destruction Associated with *S. epidermidis* Infection and Enhance Osseointegration. *Biomedicines* **2021**, *9*, 531. [[CrossRef](#)]
17. Han, J.; Yang, Y.; Lu, J.; Wang, C.; Xie, Y.; Zheng, X.; Yao, Z.; Zhang, C. Sustained release vancomycin-coated titanium alloy using a novel electrostatic dry powder coating technique may be a potential strategy to reduce implant-related infection. *Biosci. Trends* **2017**, *11*, 346–354. [[CrossRef](#)] [[PubMed](#)]
18. Zhang, L.; Yan, J.; Yin, Z.; Tang, C.; Guo, Y.; Li, D.; Wei, B.; Xu, Y.; Gu, Q.; Wang, L. Electrospun vancomycin-loaded coating on titanium implants for the prevention of implant-associated infections. *Int. J. Nanomed.* **2014**, *9*, 3027–3036.
19. Thamvasupong, P.; Viravaidya-Pasuwat, K. Controlled Release Mechanism of Vancomycin from Double-Layer Poly-L-Lactic Acid-Coated Implants for Prevention of Bacterial Infection. *Polymers* **2022**, *14*, 3493. [[CrossRef](#)]
20. Tsikopoulos, K.; Meroni, G.; Kaloudis, P.; Pavlidou, E.; Gravalidis, C.; Tsikopoulos, I.; Drago, L.; Romano, C.L.; Papaioannidou, P. Is nanomaterial- and vancomycin-loaded polymer coating effective at preventing methicillin-resistant *Staphylococcus aureus* growth on titanium disks? An in vitro study. *Int. Orthop.* **2023**, *47*, 1415–1422. [[CrossRef](#)]
21. Ma, Z.; Zhao, Y.; Xu, Z.; Zhang, Y.; Han, Y.; Jiang, H.; Sun, P.; Feng, W. 3D-printed porous titanium rods equipped with vancomycin-loaded hydrogels and polycaprolactone membranes for intelligent antibacterial drug release. *Sci. Rep.* **2024**, *14*, 21749. [[CrossRef](#)]
22. Nancy, D.; Rajendran, N. Vancomycin incorporated chitosan/gelatin coatings coupled with TiO₂-SrHAP surface modified cp-titanium for osteomyelitis treatment. *Int. J. Biolog. Macromol.* **2018**, *110*, 197–205.
23. Ordikhani, F.; Tamjid, E.; Simchi, A. Characterization and antibacterial performance of electrodeposited chitosan-vancomycin composite coatings for prevention of implant-associated infections. *Mater. Sci. Eng. C Mater. Biol. Appl.* **2014**, *41*, 240–248. [[CrossRef](#)]
24. Zarghami, V.; Ghorbani, M.; Bagheri, K.P.; Shokrgozar, M.A. Prevention the formation of biofilm on orthopedic implants by melittin thin layer on chitosan/bioactive glass/vancomycin coatings. *J. Mater. Sci. Mater. Med.* **2021**, *32*, 75. [[CrossRef](#)]
25. Vakili, N.; Asefnejad, A. Titanium coating: Introducing an antibacterial and bioactive chitosan-alginate film on titanium by spin coating. *Biomed. Tech.* **2020**, *65*, 621–630. [[CrossRef](#)]
26. Zhang, C.; Wang, Z.; Li, Y.; Yang, Y.; Ju, X.; He, R. The preparation and physiochemical characterization of rapeseed protein hydrolysate-chitosan composite films. *Food Chem.* **2019**, *272*, 694–701. [[CrossRef](#)] [[PubMed](#)]
27. Kligman, S.; Ren, Z.; Chung, C.H.; Perillo, M.A.; Chang, Y.C.; Koo, H.; Zheng, Z.; Li, C. The Impact of Dental Implant Surface Modifications on Osseointegration and Biofilm Formation. *J. Clin. Med.* **2021**, *10*, 1641. [[CrossRef](#)]
28. Catauro, M.; Papale, F.; Bollino, F. Characterization and biological properties of TiO₂/PCL hybrid layers prepared via sol–gel dip coating for surface modification of titanium implants. *J. Non-Cryst. Solids* **2015**, *415*, 9–15. [[CrossRef](#)]

29. Ferraris, S.; Örylgsson, G.; Ng, C.H.; Riccucci, G.; Spriano, S. Chemical, physical, and mechanical characterization of chitosan coatings on a chemically pre-treated Ti₆Al₄V alloy. *Surf. Coat. Technol.* **2022**, *441*, 128571. [[CrossRef](#)]
30. Pace, J.L.; Yang, G. Glycopeptides: Update on an old successful antibiotic class. *Biochem. Pharmacol.* **2006**, *71*, 968–980. [[CrossRef](#)]
31. Săndulescu, M.; Sirbu, V.D.; Popovici, I.A. Bacterial species associated with peri-implant disease—A literature review. *Germes* **2023**, *13*, 352–361. [[CrossRef](#)] [[PubMed](#)]
32. Ansari, M.; Shahlaei, M.; Hosseinzadeh, S.; Moradi, S. Recent advances in nanostructured delivery systems for vancomycin. *Nanomedicine* **2024**, *19*, 1931–1951. [[CrossRef](#)]
33. Ramya, R.; Venkatesan, J.; Kim, S.K.; Sudha, P.N. Biomedical Applications of Chitosan: An Overview. *J. Biomimetic. Biomater. Tissue Eng.* **2012**, *2*, 100–111. [[CrossRef](#)]
34. Cao, Z.; Sun, Y. Chitosan-based rechargeable long-term antimicrobial and biofilm-controlling systems. *J. Biomed. Mater. Res. A* **2009**, *89*, 960–967. [[CrossRef](#)]
35. Yang, K.; Kim, K.; Lee, E.A.; Liu, S.S.; Kabli, S.; Alsudir, S.A.; Albrahim, S.; Zhou, A.; Park, T.G.; Lee, H.; et al. Robust low friction antibiotic coating of urethral catheters using a catecholfunctionalized polymeric hydrogel film. *Front. Mater.* **2019**, *6*, 274. [[CrossRef](#)]
36. Zhou, J.; Wang, P.; Yu, D.G.; Zhu, Y. Biphasic drug release from electrospun structures. *Expert Opin. Drug Deliv.* **2023**, *20*, 621–640. [[CrossRef](#)] [[PubMed](#)]
37. Zilberman, M.; Elsner, J.J. Antibiotic-eluting medical devices for various applications. *J. Control. Release* **2008**, *130*, 202–215. [[CrossRef](#)] [[PubMed](#)]
38. Singh, M.; Lumpkin, J.A.; Rosenblatt, J. Mathematical modeling of drug release from hydrogel matrices via a diffusion coupled with desorption mechanism. *J. Control. Release* **1994**, *32*, 17–25. [[CrossRef](#)]
39. Swanson, T.E.; Cheng, X.; Friedrich, C. Development of chitosan-vancomycin antimicrobial coatings on titanium implants. *J. Biomed. Mater. Res. A* **2011**, *97*, 167–176. [[CrossRef](#)]
40. Mendoza, G.; Regiel-Futyra, A.; Tamayo, A.; Monzon, M.; Irusta, S.; de Gregorio, M.A.; Kyzioł, A.; Arruebo, M. Chitosan-based coatings in the prevention of intravascular catheter-associated infections. *J. Biomater. Appl.* **2018**, *32*, 725–737. [[CrossRef](#)]
41. McGuinness, W.A.; Malachowa, N.; DeLeo, F.R. Vancomycin Resistance in *Staphylococcus aureus*. *Yale J. Biol. Med.* **2017**, *90*, 269–281. [[PubMed](#)]
42. Niederlaender, J.; Walter, M.; Krajewski, S.; Schweizer, E.; Post, M.; Schille, C.; Geis-Gerstorfer, J.; Wendel, H.P. Cytocompatibility evaluation of different biodegradable magnesium alloys with human mesenchymal stem cells. *J. Mater. Sci. Mater. Med.* **2014**, *25*, 835–843. [[CrossRef](#)] [[PubMed](#)]
43. Amaral, I.F.; Cordeiro, A.L.; Sampaio, P.; Barbosa, M.A. Attachment, spreading and short-term proliferation of human osteoblastic cells cultured on chitosan films with different degrees of acetylation. *J. Biomat. Sci. Polym. Ed.* **2007**, *18*, 469–485. [[CrossRef](#)] [[PubMed](#)]
44. Braun, J.; Eckes, S.; Rommens, P.M.; Schmitz, K.; Nickel, D.; Ritz, U. Toxic Effect of Vancomycin on Viability and Functionality of Different Cells Involved in Tissue Regeneration. *Antibiotics* **2020**, *9*, 238. [[CrossRef](#)]

Disclaimer/Publisher’s Note: The statements, opinions and data contained in all publications are solely those of the individual author(s) and contributor(s) and not of MDPI and/or the editor(s). MDPI and/or the editor(s) disclaim responsibility for any injury to people or property resulting from any ideas, methods, instructions or products referred to in the content.